Available online at www.sciencedirect.com

ScienceDirect

Procedia Engineering 10 (2011) 3032–3037

Engineering Procedia

ICM11

Equivalent Young's Modulus of the Spiral Accumulating Motor Core Including Many Slits and Embossing Interlockings*

N.-A. Noda[a], Y. Takase[a] and H. Takada[a]*

[a] *Department of Mechanical Engineering, Kyushu Institute of Technology, 1-1 Sensui-Cho, Tobata-Ku, Kitakyushu, 804-8550 Japan*

Abstract

The motor core is usually manufactured from magnetic steel sheet with press machine. However, usually most parts of the plate are scalped, and only small percent of the sheet is used for the core. The spiral accumulating core system is suitable for manufacturing the core more ecologically because in this system more than 50% of the magnetic steel sheet can be used. However, since the spiral accumulating core has many slits and embossing interlockings, the equivalent Young's modulus is not known. In this study, therefore, the equivalent Young's modulus of the spiral accumulating core is considered in order to find out a good method to fix the core. Here, the finite element method is applied to analyze the permanent magnet motor core, whose layers and slits are periodically arranged. Then, the effects of slits, layers and embossing interlockings on equivalent Young's modulus are discussed. It is found that around the slits the core layer should be considered to have zero elastic modulus because no tangential stress exists. Finally, a convenient method of calculation based on rule of mixture is newly proposed to estimate the equivalent Young's modulus efficiently.

Keywords:spiral, accumulating, finite element method, bending, deterioration

1. Introduction

The motor core is usually manufactured from magnetic steel sheet [1] with press machine. However, usually most parts of the plate are scalped, and only small percent of the sheet is used for the core. Therefore the conventional manufacturing method is not suitable for large diameter motors core in terms of ecology. On the other hand, the spiral accumulating core system [2]-[6] is suitable for manufacturing the core more ecologically because in this system more than 50% of the magnetic steel sheet can be used (see Fig.1).

In this analysis, equivalent Young's modulus is considered for spiral accumulating core used for permanent magnet motor by the application of the finite element method to 3D models, whose layers and slits are periodically arranged. Then, effects of slits, layers and embossing interlockings on equivalent Young's modulus are analyzed. Finally, a convenient method of calculation based on the rule of mixture is newly proposed for estimating the equivalent Young's modulus of the real spiral accumulating core. Here, we considered the PM synchronous motor,

* N.-A. Noda. Tel.: +81-93-884-3124; fax: +81-93-884-3124.
E-mail address: noda@mech.kyutech.ac.jp.

1877-7058 © 2011 Published by Elsevier Ltd. Open access under CC BY-NC-ND license.
Selection and peer-review under responsibility of ICM11 doi:10.1016/j.proeng.2011.04.502

which is a rotating electric machine where the stator is a classic three phase stator like that of an induction motor and the rotor has surface-mounted permanent magnets. Recently, permanent magnet motors are widely used in wide industrial fields because they are suitable for compact mechanical system. The present study is also useful for in-wheel motor become those motors has large diameters.

2. Method of analysis

Figure 2 shows (a) axis and rotor and (b) housing and stator after shrink fitting. The compressive stress always acts in the circumferential direction when the stator is fixed on the outside housing. Since the slit sustains the compressive stress, there is little effect on the Young's modulus. However, when the rotor is fixed on the axis, the tensile stress appears in the circumference direction; and therefore it is necessary to analyze the equivalent Young's modulus for rotor in order to fix it properly.

Figure 3 shows three types of layers, A, B, C. Assume three layers are in the range of $\theta = 36^\circ - 90^\circ$ (see Fig.5). For example, each layer of core shape in the range of $90^\circ - 144^\circ$ coincide with that in the range of $36^\circ - 90^\circ$. The fourth layer is the same as the first layer. Using the model, the equivalent Young's modulus of the spiral accumulating core is evaluated by applying the finite element method to this model.

Figure 4 shows the example of FEM mesh for 3D model. In this study, the linear hexahedron element is used. The total number of elements is 60450, and total number of nodes is 77868. As shown in Fig.4, each layer is combined together at each embossing interlockings; and therefore the circumferential force is transferred by those embossing interlockings near the slits. Figure 5 shows the boundary conditions of the model. As shown in Fig.5, the displacement in the θ direction at $\theta = 36^\circ$ is fixed, and displacement in the θ direction at $\theta = 90^\circ$ is fixed, that is, $u_\theta=0$ at $\theta=36^\circ, 90^\circ$. We have also considered the results periodic boundary conditions are applied at $\theta=36^\circ$ and 90°. It is confirmed that the results for the periodic boundary conditions and fixed conditions are almost the same. The displacement in the z direction is fixed as both $u_z=0$ at the top of surface on the 1st layer and bottom of surface on the 3rd layer. Then the constant displacement in the r-direction $u_r=\Delta R$ is given at r = R (see Fig.5).

Fig.1 Automatic spiral accumulating

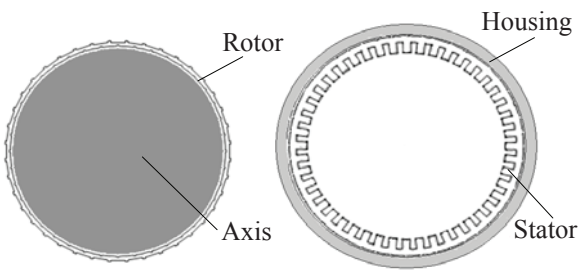

(a) (b)

Fig.2 Shrink fit for (a) rotor and (b) stator

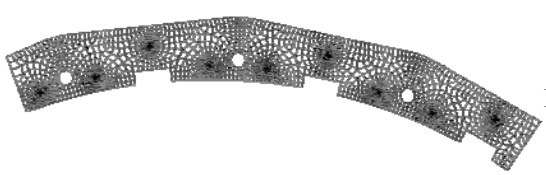

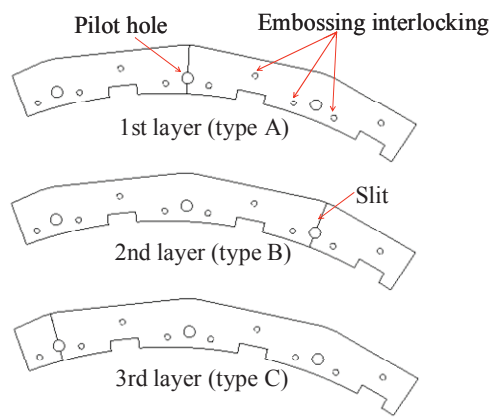

Fig.3 Three types of layers

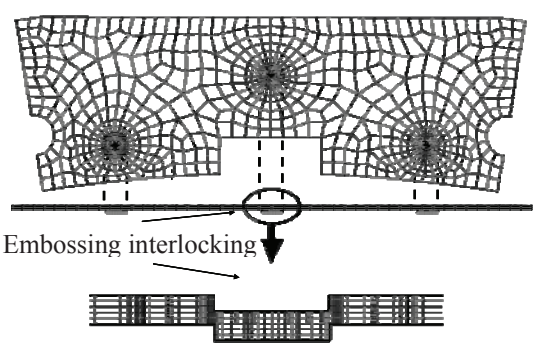

Fig.4 Example of FEM mesh for 3D model

The equivalent Young's modulus of the 3D dimensions model is given by Eq. (1).

$$E^* = \frac{\sigma_{\theta av}}{\varepsilon_\theta} = \frac{\sigma_{\theta 1} + \sigma_{\theta 2} + \sigma_{\theta 3}}{3(\Delta R / R)} \tag{1}$$

In Fig.6, $\sigma_{\theta 1}$, $\sigma_{\theta 2}$, $\sigma_{\theta 3}$ are the average stress of first layer, second layer and third layer of the model respectively, the stress $\sigma_{\theta av}$ is the average stress of three layer accumulating model, and ε_θ is a strain of the direction of θ, and the value is equal to the strain value of the direction of R. Moreover, R is a radius in the core, and ΔR is constant displacement in the radial direction. It should be noted that the average stress of each layer is considered at the inside of each core because of the shrink fitting (see Fig.6(a)). In other words, equivalent Young's modulus should be considering at the inside of the core.

3. Results and discussion

It is not suitable to consider the real core shape when we discuss the effect of fundamental geometrical conditions on the equivalent Young's modulus because the core shape is too complicated. Therefore, simple shape of core models as shown in Fig.7 (b) is considered whose interval is 60 degree. In Fig.7, the thickness of the core is illustrated in a large scale in order to show the positions of the slits clearly. It should be noted that the real core thickness is only about 0.5mm.

First, the effect of core shape difference is considered as shown in Fig.8. There are several differences between the real core A and simple core D, for example pilot hole, notch, etc. Here, the effect of each difference on the equivalent Young's modulus E* is investigated. Figure 8 shows the equivalent Young's modulus for each model A, B, C, D. It is seen that the equivalent Young's modulus of Model A is smaller than that of Model C by 16%.

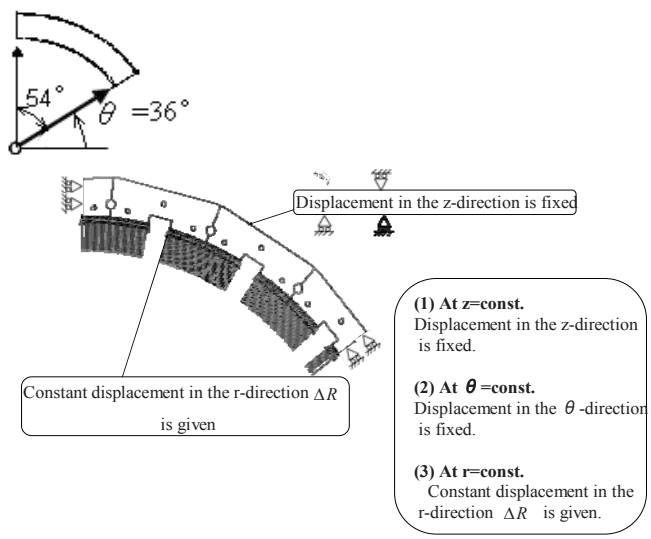

Fig.5 Boundary conditions of the model

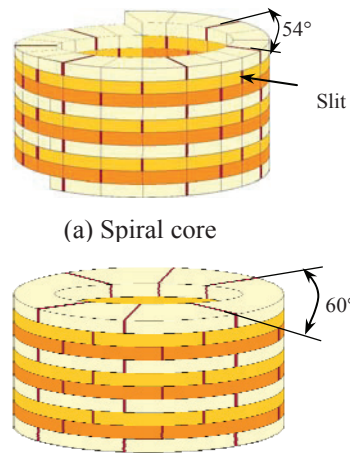

(a) Spiral core

(b) Conventional layered core

Fig.7 Diagrammatic illustration of rotor core (thickness enlarged)

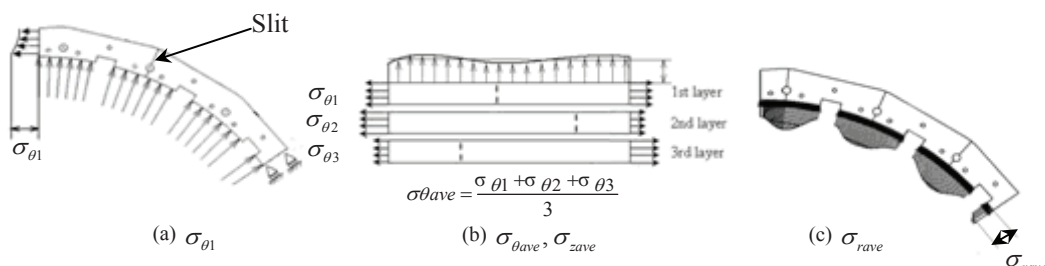

(a) $\sigma_{\theta 1}$ (b) $\sigma_{\theta ave}, \sigma_{zave}$ (c) σ_{rave}

Fig.6 Definition of $\sigma_{\theta ave}, \sigma_{zave}, \sigma_{rave}$

Figure 9 shows the example of simple two layer's model. The second layer has phase difference of two embossing interlockings from the first layer. Here, 60°model as shown in Fig.7 is used to approximate 54°spiral model because each layer can be separated and can be investigated more easily.

3.1 Effect of number of interlocking n_s between slits on the equivalent Young's modulus

In this analysis, two layers models are considered. Then, the number of interlocking n_s on equivalent Young's modulus E* is calculated. It is assumed that the number of slits Ns=6. Figure 10 shows simple layer's model when n_s = 2 and 4. Table 1 shows relationship between E* and ns. Equivalent Young's modulus becomes constant when number of n_s = 3, 4 and 5. In the case of simple two layer's model, effect of number interlocking ns on the equivalent Young's modulus become larger.

3.2 Effect of number of slits Ns on the equivalent Young's modulus

Effects of width and diameter will be considered with varying number of slits. In this analysis, the number of interlocking n_s between the slits is fixed as $n_s = 2$. Then, the number of slits are changed as N_S=1, 2, 3, 6, 12. Three analysis models of FEM are calculated. (1)Basic Model has dimension t=16mm, (2) Two times width Model has dimension t=32mm, (3) Two times diameter Model has dimension D=284mm.

Figure 11 and Table 2 shows relation between equivalent Young's modulus E* and number of slits Ns. Equivalent Young's modulus E* decreases with increasing of number of slits. Equivalent Young's modulus E* of wide core becomes small. E* of large diameter becomes large.

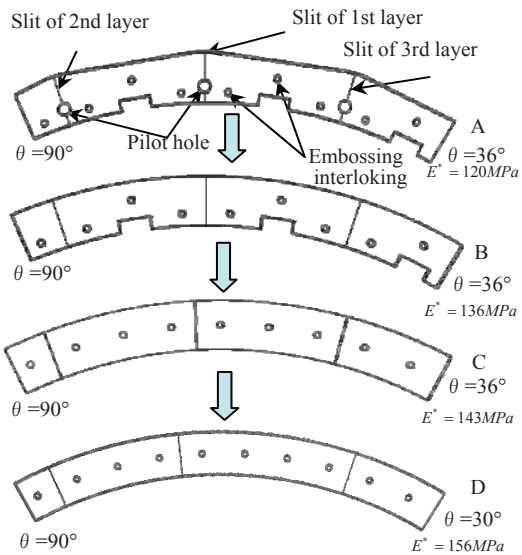

Fig.8 Real core A and simple core D

Table 1 Effect of n_s on E^*

Number of embossing interlocking n_s	Equivalent Young's modulus E^* [GPa]
n_s =1	122.5
n_s =2	138.3
n_s =3	144.0
n_s =4	145.0
n_s =5	144.0

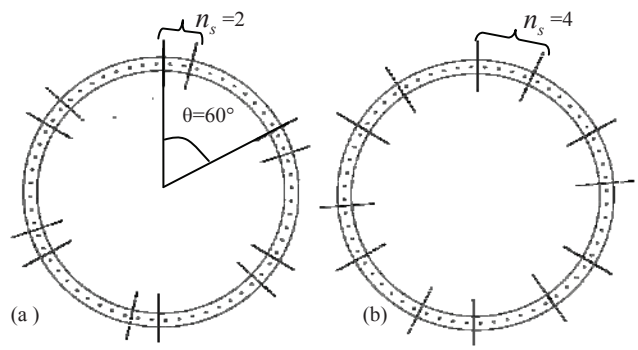

Fig.10 Effect of ns on E^* (a) n_s =2 (b) n_s =4
n_s :Number of embossing interlocking between 1st and 2n layers

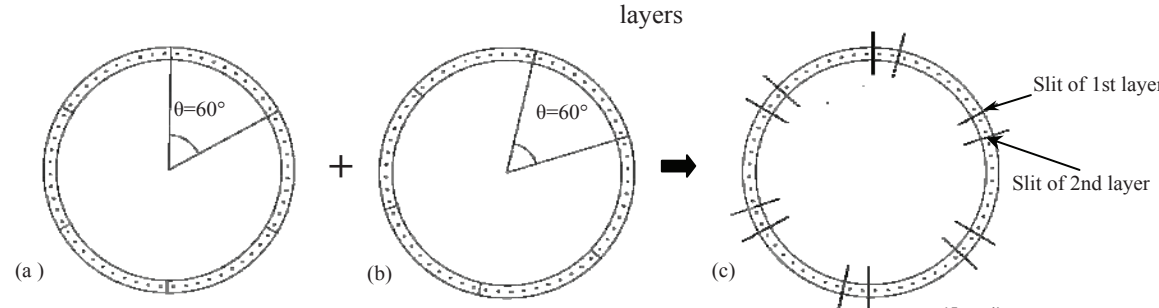

Fig.9 (a) First layer with slits at θ= $\frac{n\pi}{3}$ (n=0,1,2,3,4,5), (b) Second layer with slits at θ=$\frac{(5n+1)\pi}{15}$ (n=0,1,2,3,4,5), (c) Two layers are fixed at embossing interlocking

4 Simple calculation method based on rule of mixture

4.1 Rule of mixture to evaluate the equivalent Young's modulus E*

Figure 12 shows an example of two layers model whose layer has phase difference of distance for two embossing interlocking. In this example each layer has six slits. Figure12 (d) and Figure 13 show unit cell model for 60degree interval. Figure 13(a) shows detail view of Fig.7(b) from the z-direction. Figure 13(b) shows the detail view of Fig.7(b) from the r-direction. Since the grey region (block2) has almost no stress due to the slits, block2 can be regard as a single layer as shown in Fig. 13 (c) ($E_2=E_o/2$). Equation (2)shows the rule of mixture for series model. Here, the values E_0 =206GPa and E_2=103GPa[$E_2=E_0/2$] are Young's modulus for block1 and block2, respectively.

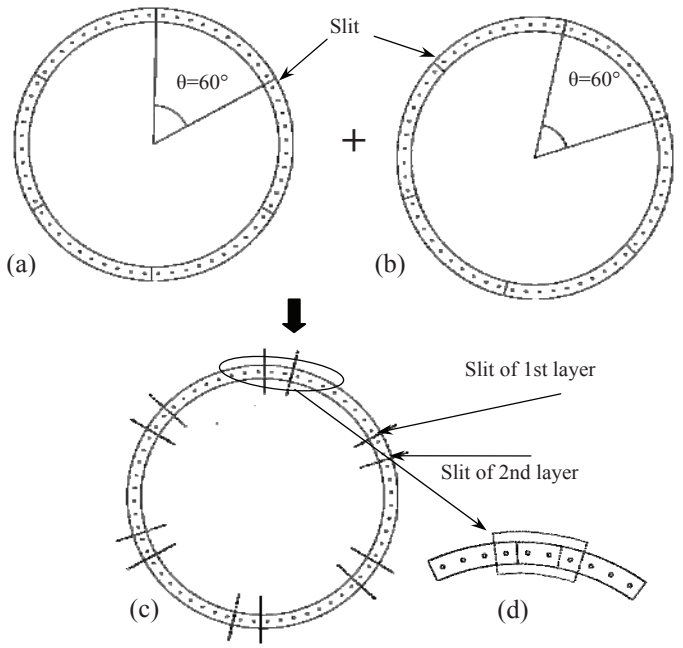

Fig.12 Two layer's model of spiral core
(a) First layer with slits at $\theta=\frac{n\pi}{3}$, n=0,1,2,3,4,5),
(b) Second layer with slits at $\theta=\frac{(5n+1)\pi}{15}$, n=0,1,2,3,4,5),
(c) Two layers are fixed at embossing interlockings, (d)Unit cell

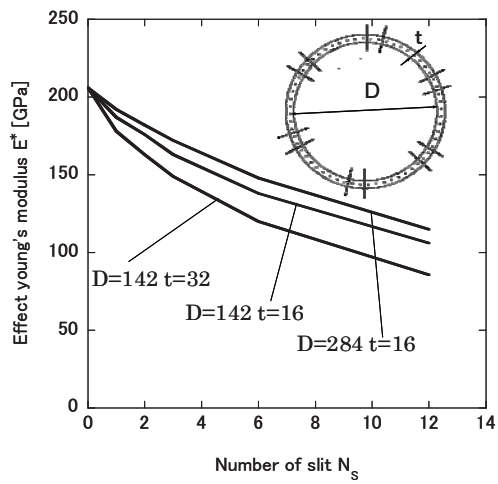

Fig.11 Effect of number of slit N_S on E^*

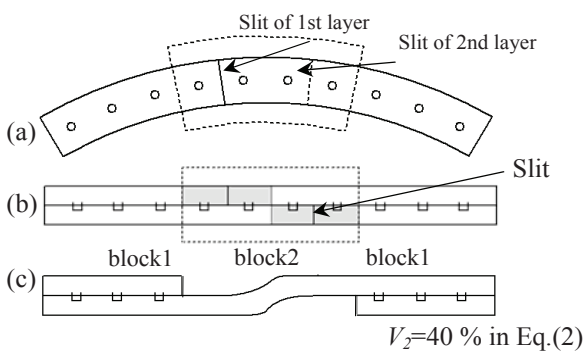

V_2=40 % in Eq.(2)

Fig.13 Unit cell of two layer's model
(a) Two layers model , (b) Positions of silts ,
(c) Approximation method

Table 2 Effect of number of slit N_S on E^*
(N_S : Effect of number of slit of one layer)

N_s	Equivalent Young's modulus E^*[GPa]		
	D=142[mm] t=16[mm]	D=142[mm] t=32[mm]	D=284 [mm] t=16[mm]
12	**106**	**85.6**	**115**
6	**138**	**120**	**148**
3	**163**	**149**	**172**
2	**176**	**163**	**182**
1	**187**	**178**	**192**

$$E^* = \frac{E_2 E_o}{E_o V_2 + (1 - V_2) E_2} \quad (2)$$

E^*: Equivalent Young's modulus, E_o:block1's Young's modulus, E_2 :block2's Young's modulus, V_2 :block2's volume fraction

4.2 Evaluation for equivalent Young's modulus E* of real spiral accumulating core

As shown in Table 3, the equivalent Young's modulus is analyzed by applying the finite element method to 3D model of the simple shape of core. And, Table 3 shows the values of the rule of mixture in eq. (2). Estimating the equivalent Young's modulus can be given by using the rule of mixture in eq. (2) with less than 10% error. Table 4 shows the results for equivalent Young's modulus of block2. As shown in Table 4 it is found that the results of rule of mixture $E_2 \fallingdotseq E_o/2$=103 GPa has 18% error from the results of FEM.

Here, a convenient method of calculation based on rule of mixture is newly proposed to estimate the Young's modulus of the real spiral accumulating core efficiently. First, a convenient method of calculation can be applied to 3 layer's model. In Fig. 14, block2 has two layers. Block1 has three layers. E_2 of block2 is 137GPa. E* is obtained by this equation. By using rule of mixture, simple shape core can be estimated within 16% error. Next, from the Figure 15, E* of real core is smaller than that of simple core by 16%. On the basis of the rule of mixture, simple core's E* can be calculated. Real E* can be estimated from the results of finite element method. Rule of mixture has accuracy within 6% error.

5. Conclusions

In this study, equivalent Young's modulus of spiral accumulating core used for permanent magnet motor is discussed by the application of the finite element method. The convenient method of calculation based on the rule of mixture is newly proposed to estimate the Young's modulus of the real spiral accumulating core efficiently.

References

[1] Kaido, C. Spiral Core made of Grain-oriented Electrical Steel Sheet. IEEJ Transactions on Industry Applications, 1996; 116- 3, p. 265-270

[2] Abb research ltd. Method of forming motor, Japan patent (in Japanese), 2004-505595.

[3] Kumai, S., and Yaskawa electric corp. Winding accumulating core of motor, Japan patent (in Japanese), s51-40506.

[4] Kikuchi, Y., Fukuda, Y., Maeyama, K., and Fujitsu general ltd. :Motor, Japan patent, 2005-160170.

[5] Sakanishi, S., Asai, T., Koyama, M., and Kuroda precision ind. ltd., Mitsuba electric mfg. co. ltd. : Method and device for manufacturing winding stator core, Japan patent, h2-106151.

[6] Mizutani, K., and Toshiba corp.: Manufacture of annular core, Japan patent, h1-264548.

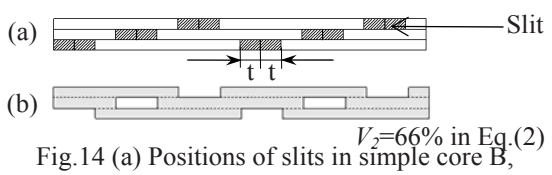

Fig.14 (a) Positions of slits in simple core B, (b) Approximation method

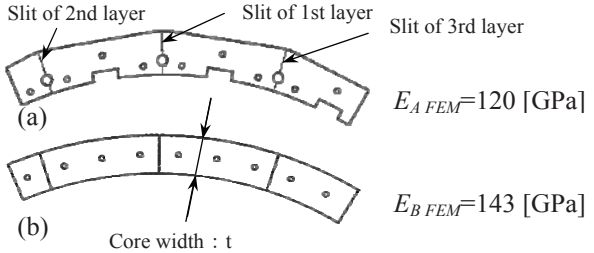

Fig.15 Difference between real core A and simple core B (a) Real core model A, (b) Simple core model B

Table 3 Effect of number of slit N_S on E^* (N_S : Effect of number of slit of one layer)

Ns	Equivalent Young's modulus E^*[GPa]					
	D=142[mm] t=32 [mm]		D=142[mm] t=16 [mm]		D=284[mm] t=16 [mm]	
	FEM	ROM	FEM	ROM	FEM	ROM
12	85.6	90.4	106	113	115	128
6	120	126	138	146	148	158
3	149	157	163	171	172	179
2	163	170	176	181	182	187
1	178	186	187	193	192	196

Table 4 Equivalent Young's modulus E^* of block2 in Fig.13 ($E^*_{ROM} = 103GPa$)

Ns	Equivalent Young's modulus E^*[GPa]		
	D=142[mm] t=16[mm]	D=142[mm] t=32[mm]	D=284 [mm] t=16[mm]
12	95.8	97.0	92.1
6	95.1	96.1	94.0
3	93.6	92.7	93.8
2	94.3	91.3	93.8
1	84.2	85.6	93.7